Quantum Inf Process
DOI 10.1007/s11128-012-0445-0

Differential topology of adiabatically controlled quantum processes

Edmond A. Jonckheere · Ali T. Rezakhani · Farooq Ahmad

Received: 6 February 2012 / Accepted: 20 June 2012

Abstract It is shown that in a controlled adiabatic homotopy between two Hamiltonians, H_0 and H_1, the gap or "anti-crossing" phenomenon can be viewed as the development of cusps and swallow tails in the region of the complex plane where two critical value curves of the quadratic map associated with the numerical range of $H_0 + iH_1$ come close. The "near crossing" in the energy level plots happens to be a generic situation, in the sense that a crossing is a manifestation of the quadratic numerical range map being unstable in the sense of differential topology. The stable singularities that can develop are identified and it is shown that they could occur near the gap, making those singularities of paramount importance. Various applications, including the quantum random walk, are provided to illustrate this theory.

Keywords Adiabatic theorem · Numerical range · Cusps · Swallow tails · Gap · Anti-crossing

1 Introduction

Adiabatic computers appear promising as demonstration test-beds of quantum computations, probably because instead of going for universality they rather target a

E. A. Jonckheere (✉)
USC Center for Quantum Information Science & Technology, Los Angeles, CA 90089, USA
e-mail: jonckhee@usc.edu

A. T. Rezakhani
Sharif University of Technology, Teheran, Iran
e-mail: rezakhani@sharif.edu

F. Ahmad
Delta Tau Data Systems, Inc., Chatsworth, CA 91311, USA
e-mail: fahmad@deltatau.com

Published online: 02 September 2012

well-defined generic problem: the computation of the ground state $|\psi_1\rangle$ of a system with "complicated" $N \times N$ Hamiltonian H_1. The solution proceeds from an easily computable ground state $|\psi_0\rangle$ of a system H_0, followed by a continuation to $|\psi_1\rangle$. Continuation methods have been around for a while, but what makes adiabatic computations so specific is that the continuation from the "easy" to the "difficult" problem is provided by Schrödinger's equation. Specifically, a controlled homotopy from H_0 to H_1 is set up as $H(t) = H_0 u_0(t) + H_1 u_1(t)$ with $H(0) = H_0$ and $H(1) = H_1$, the initial condition $|\psi(0)\rangle$ on Schrödinger's equation $\partial|\psi(t)\rangle/\partial t = -iH(t)|\psi(t)\rangle$ is prepared as the ground state $|\psi_0\rangle$ of H_0, with the hope that the fidelity $|\langle\psi_1|\psi(1)\rangle|^2 \approx 1$. This adiabatic behavior is guaranteed provided the homotopy is so slow as to satisfy

$$\max_{t\in[0,1]} \frac{|\langle\psi_k(t)|\dot{\psi}(t)\rangle|^2}{(E_k(t) - E_1(t))^2} \ll \min_{t\in[0,1]} (E_k(t) - E_1(t)), \quad k = 2, ..., N,$$

where $H(t)|\psi_k(t)\rangle = E_k(t)|\psi_k(t)\rangle$ and the $E_k(t)$'s are the various energy levels (eigenvalues) of $H(t)$ listed as $E_1(t) < E_2(t) \leq E_3(t) \leq \cdots \leq E_N(t)$ (see [1, Eqs. (7), (10)]).

Clearly, the most constraining feature is the "gap," $\min_t(E_2(t) - E_1(t))$. It turns out that a small gap is a *generic* phenomenon that results from the bifurcation of the unstable singularity of eigenvalue crossing to a stable "anti-crossing." Here "stable" means that, under data perturbation, the repelling effect of E_1 on E_2 and vice versa remains persistent. Symmetry in general creates unstable eigenvalue crossings, while under symmetry breaking the crossings bifurcate to stable anti-crossings (see Sect. 5.1). In such simple cases as adiabatic Grover's search (see Sect. 3.1), the anti-crossing is a singularity that can be analyzed locally. However, in more complicated cases, e.g., Ising chains (see Sect. 5), the anti-crossing is inextricably intertwined with nearby "swallow tails" phenomena, necessitating a *global, topological* view on the singularities. Singularity theory can loosely be defined as the study of smooth maps under rank deficient matrix of partial derivatives. The global analysis of the rank drops of relevant Jacobian matrices is the field of differential topology.

Naturally, the homotopy control $(u_0(t), u_1(t))$ determines the singularities that can be encountered. How to control the homotopy has been the subject of various investigation, but mainly from the point of view of time-optimization of the computation given the constraints of the adiabatic theorem [2,3]. The ultimate objective of our work is rather to control the singularities. More specifically, here, we would like to single out all singularities that could potentially be encountered for any homotopy from H_0 to H_1. To achieve this objective, we devise a generic homotopy from H_0 to H_1 and back to H_1 as $H(t) = H_0 \cos(\pi t/2) + H_1 \sin(\pi t/2)$. The plots of the eigenvalues of $H(t)$ immediately show near-crossings. The crucial step necessary to acquire a global vision on the problem is to encode the energy level plots as critical value curves of a quadratic mapping defined on the unit sphere $f : \mathbf{z} \mapsto \langle\mathbf{z}|H_0 + iH_1|\mathbf{z}\rangle$. This "encoding" is developed in Sect. 2. The image of this mapping, $f(S^{2N-1})$, is the numerical range of the matrix $H_0 + iH_1$, so that the adiabatic theorem boils down to the differential topology of the numerical range of $H_0 + iH_1$ in the sense of [4]. For clarity of the exposition, the later is briefly reviewed in Sect. 2.2.

The paper then proceeds with such simple examples as Grover's search (Sect. 3.1) and the inversion of Toeplitz matrices (Sect. 3.2). After a topological interlude where swallow tails and cusps are defined (Sect. 4), we are in a position to come to the more complicated case of Ising chains (Sect. 5). Finally, the far from trivial case of adiabatic computation of quantum hitting time is developed in Sect. 6. The conclusion develops the concept of "navigation in a sea of singularities."

2 Basic concepts, definitions, and results

Consider an adiabatic homotopy $H(u_0(t), u_1(t)) = u_0(t)H_0 + u_1(t)H_1$, where the initial and terminal Hamiltonians, H_0, H_1, are Hermitian matrices of size N, the homotopy parameter $t \in [0, 1]$, and the initial and terminal conditions are $u_0(0) = u_1(1) = 1$, and $u_0(1) = u_1(0) = 0$. The eigenvalues of $H(u_0(t), u_1(t))$ are the energy levels and they are well known to "nearly cross," requiring the adiabatic algorithm to slow down through the gap. This phenomenon was apparently singled first by von Neumann and Wigner [5]. Our main point is that the plots of the eigenvalues (energy levels) are the plots of the critical values of a quadratic map associated with $H(u_0(t), u_1(t))$. This supports our point that the adiabatic gap is indeed a differential topological issue, since differential topology mainly deals with the study of the critical points and the critical values of smooth maps.

2.1 A generic homotopy

To illustrate the ideas, we set up the homotopy as $u_0(t) = \cos(\pi t/2)$ and $u_1(t) = \sin(\pi t/2)$. The main point linking the adiabatic theorem to differential topology is the fact—proved in [4] and generalized in [6]—that $\forall t \in \mathbb{R}$ the eigenvalues (eigenvectors) of $H_0 \cos(\pi t/2) + H_1 \sin(\pi t/2)$ are the critical values (critical points) of the $\mathbb{R}$-valued quadratic map

$$f_{\frac{\pi t}{2}} : S^{2N-1}/S^1 \cong \mathbb{CP}^{N-1} \to \mathbb{R}$$
$$|\mathbf{z}\rangle \mapsto \langle \mathbf{z}| \big(H_0 \cos(\pi t/2) + H_1 \sin(\pi t/2)\big) |\mathbf{z}\rangle.$$

The reason for the subscript $\frac{\pi t}{2}$ will become clearer later. The domain of $f_{\frac{\pi t}{2}}$ is the quotient of the unit sphere S^{2N-1} of $\mathbb{C}^N$ by the unit circle S^1 to remove the ambiguity of the phase factor of $\|\mathbf{z}\| = 1$. The quotient S^{2N-1}/S^1 is well known to be the complex projective space $\mathbb{CP}^{N-1}$. Recall that a *critical point* is a point z^0 where the differential $d_{z^0} f_{\frac{\pi t}{2}} : T_{z^0}\mathbb{CP}^{N-1} \to \mathbb{R}$ vanishes. The corresponding *critical value* is $f_{\frac{\pi t}{2}}(z^0)$.

In order to visit *all* angles and as such exhibit *all* potential singularity phenomena, we extend the homotopy from $t \in [0, 1]$ to $t \in [0, 4]$. It we set $\theta = \pi t/2$, the homotopy is extended from $\theta \in [0, \pi/2]$ to $\theta \in [0, 2\pi]$. In other words, we devise a homotopy from H_0 to H_1 and then back to H_0 along a circle in the span(H_0, H_1) plane of the space of Hermitian matrices. Having a loop in the space of $N \times N$ Hermitian matrices allows us to determine whether two paths between H_0 and H_1 can be deformed

without encountering eigenvalue crossing obstructions. (The same obstructions have to be avoided when an open quantum system is controlled in such a way as to preserve a subset of eigenvalues of the density operator, while the complementary eigenvalues are allowed to change, but without crossing. The system is then said to evolve in a "decoherence-splitting manifold" [7].)

2.2 Differential topology of numerical range: a review

The critical values of a homotopy of Hermitian matrices of the form $H_0\cos(\pi t/2) + H_1\sin(\pi t/2)$, properly extended to $t \in [0, 4]$, are closely related to the *numerical range* or *field of values* $\mathcal{F}$ of the matrix $H_0 + iH_1$, defined as the image $f(\mathbb{CP}^{N-1})$ of the $\mathbb{C}$-valued quadratic map

$$\begin{aligned} f : \mathbb{CP}^{N-1} &\to \mathbb{C} \\ |\mathbf{z}\rangle &\mapsto \langle \mathbf{z}|(H_0 + iH_1)|\mathbf{z}\rangle. \end{aligned}$$

By the Toeplitz–Hausdorff theorem, the numerical range is a closed, convex subset of $\mathbb{C}$. The connection between the two maps is easily seen to be $f_{\pi t/2}(|\mathbf{z}\rangle) = \Re(f(|\mathbf{z}\rangle)\exp(-\pi t/2))$, which means that $f_{\pi t/2}(|\mathbf{z}\rangle)$ can be read out by projecting $f(|\mathbf{z}\rangle)$ on the line with argument θ, as shown in Fig. 2.

The $\mathbb{C}$-valued quadratic map of the numerical range also has critical points and critical values. The *critical points* are those points $|\mathbf{z}^0\rangle$ where the rank (over $\mathbb{R}$) of the differential $d_{|z^0\rangle}f : T_{|z^0\rangle}\mathbb{CP}^{N-1} \to \mathbb{C}$ drops (below 2) and the corresponding *critical values* are $f(|\mathbf{z}^0\rangle)$. From Sard's theorem [8, Chap. II], the critical value set is of zero measure in $\mathbb{C}$.

A property of a $N \times N$ complex matrix viewed as a point in $\mathbb{C}^{N\times N}$ is said to be *generic* if the set of matrices enjoying that property is *open and dense* in $\mathbb{C}^{N\times N}$. No eigenvalue crossings in the family $H_0\cos(\pi t/2) + H_1\sin(\pi t/2)$ is a generic property. Smoothness of the boundary $\partial\mathcal{F}$ of the field of values is also generic. Among non-generic features, one will retain sharp points $f(|\mathbf{z}^0\rangle)$ in $\partial\mathcal{F}$, which are rank 0 critical values, in the sense that $\operatorname{rank}(d_{|z^0\rangle}f) = 0$. A line segment embedded in $\partial\mathcal{F}$ consists of rank 0 critical value points. A smooth boundary point, on the other hand, is a rank 1 critical value in the sense that $\operatorname{rank}(d_{|z^0\rangle}f) = 1$. (See Sect. 4 and the sharp point $1 + i$ of Fig. 2 for an illustrative example.)

The difficulty is that, in addition to the boundary, the interior of the numerical range contains other *nonsmooth* critical value curves exhibiting such typical singularity phenomena as swallow tails and cusps. Swallow tails and cusps are generic; they persist under data perturbation. A generic singularity is also said to be stable. (The reader is referred to [4,9] for details of the specific case of the singularities of the critical value curves of the numerical range, to [10–12] for the general theory of singularities, and to [13] for the general theory of singularities of curves and caustics.)

The connection between the critical values of the $\mathbb{R}$- and the $\mathbb{C}$-valued maps is easily understood by observing that the projection of $\langle \mathbf{z}|(H_0 + iH_1)|\mathbf{z}\rangle$ on the line with argument $\pi t/2$ is $(H_0\cos(\pi t/2) + H_1\sin(\pi t/2))\exp(i\pi t/2)$. As such, those points on the boundary $\partial\mathcal{F}(H_0 + iH_1)$ with their tangent of argument $\pi t/2 \pm \pi/2$

will project as critical (extremal) values of $\langle \mathbf{z}| \left(H_0 \cos(\pi t/2) + H_1 \sin(\pi t/2)\right) |\mathbf{z}\rangle$. A more refined analysis (see [4] for details) reveals that any tangent at an argument $\pi t/2 \pm \pi/2$ to any critical value curve in the interior of $\mathcal{F}(H_0 + i H_1)$ will also project as a (nonextremal) critical value of $\langle \mathbf{z}| \left(H_0 \cos(\pi t/2) + H_1 \sin(\pi t/2)\right) |\mathbf{z}\rangle$. The converse is also true: the envelope of the lines at an argument $\pi t/2 \pm \pi/2$ and at a distance $\langle \mathbf{z}^0| \left(H_0 \cos(\pi t/2) + \sin(\pi t/2)\right) |\mathbf{z}^0\rangle$ from the origin are critical value curves of $\langle \mathbf{z}| \mapsto \langle \mathbf{z}|(H_0 + i H_1)|\mathbf{z}\rangle$.

2.3 General homotopy

As stated earlier, for illustration purposes, the homotopy was set up as $u_0(t) = \cos(\pi t/2)$ and $u_1(t) = \sin(\pi t/2)$. We now show that the same paradigm holds for an arbitrary homotopy, e.g., the well known homotopy $u_0(t) = 1-t$ and $u_1(t) = t$. Under a general homotopy $H_0 u_0(t) + H_1 u_1(t)$ in $P_{01} = \text{span}(H_0, H_1) \subset \text{Herm}(N \times N)$, stable and occasionally unstable singularities will be encountered. Stable singularities are omnipresent. Unstable singularities of all quadratic maps of all $H \in \text{Herm}(N \times N)$ are in the so-called discriminating set $\mathcal{D}$. The latter breaks into several strata, each of which separates two path-connected domains of stable singularities. Thus, under a general homotopy $H_0 u_0(t) + H_1 u_1(t)$, the unstable singularities will be confined to $P_{0,1} \cap \mathcal{D}$. If we recall that a critical point is an eigenvector of $H_0 u_0 + H_1 u_1$, the same point is also critical for the quadratic map of $(H_0 u_0 + H_1 u_1)/\|u\|^2 = (H_0 \cos\theta + H_1 \sin\theta)$ after obvious change of variable. We are clearly back to the generic homotopy after scaling the energy level by a factor of $\|u\|^2$. If $\|u(t)\|^2$ is smooth, it will not change the singularity structure.

3 First applications

In a number of applications, the initial and final Hamiltonians are of the form $H_0 = I - |\mathbf{a}\rangle\langle\mathbf{a}|$ and $H_1 = I - |\mathbf{b}\rangle\langle\mathbf{b}|$, where $\|\mathbf{a}\| = \|\mathbf{b}\| = 1$ and I is the identity matrix. Without loss of generality, we can take $|\mathbf{b}\rangle = \alpha_0 |\mathbf{a}\rangle + \alpha_1 |\mathbf{a}_1^\perp\rangle$, where $\langle \mathbf{a}|\mathbf{a}_1^\perp\rangle = 0$ and $\|\mathbf{a}_1^\perp\| = 1$, whence

$$\alpha_0 = \langle \mathbf{a}|\mathbf{b}\rangle, \quad \alpha_1 = \sqrt{1 - |\alpha_0|^2}, \tag{1}$$

and

$$\begin{aligned} H(u_0, u_1) &= \begin{pmatrix} u_1|\alpha_1|^2 & -u_1\alpha_0\bar{\alpha_1} \\ -u_1\alpha_1\bar{\alpha_0} & u_0 + u_1|\alpha_0|^2 \end{pmatrix} \oplus (u_0 + u_1) I_{N-2} \\ &= u_0 \left(\begin{array}{cc|c} 0 & 0 & 0 \\ 0 & 1 & 0 \\ \hline 0 & 0 & I_{N-2} \end{array}\right) + u_1 \left(\begin{array}{cc|c} |\alpha_1|^2 & -\alpha_0\bar{\alpha}_1 & 0 \\ -\bar{\alpha}_0\alpha_1 & |\alpha_0|^2 & 0 \\ \hline 0 & 0 & I_{N-2} \end{array}\right). \end{aligned}$$

Therefore, the relevant numerical range problem is that of the matrix

$$\left(\begin{pmatrix}0 & 0\\ 0 & 1\end{pmatrix} + i\begin{pmatrix}|\alpha_1|^2 & -\alpha_0\bar{\alpha}_1\\ -\bar{\alpha}_0\alpha_1 & |\alpha_0|^2\end{pmatrix}\right) \oplus (1+i)I_{N-2}.$$

It is thus the numerical range of the direct sum of two matrices. This numerical range is the convex hull of the numerical range of the first term and that of the second term of the direct sum. The numerical range of $(1+i)I_{N-2}$ is just the singleton $\{1+i\}$, but of multiplicity $N-2$. Its $\exp(i\theta)$-projection is obviously $\cos\theta + \sin\theta$, hence a cosine/sine curve in the plot of critical values (energy levels). Next to this cosine/sine curve, there will be the $\exp(i\theta)$-projection of the boundary of the numerical range of the first term of the direct sum. The numerical range of this 2×2 matrix is well known to be an ellipse, and it can be further shown—see Sect. 3.3—that its principal axes are at a $\pm 45°$ angle with the real axis, Fig. 2.

From the specific point of view of the adiabatic theorem, an important issue is whether

$$\{1+i\} \in \mathcal{F}\left(\left(\begin{pmatrix}0 & 0\\ 0 & 1\end{pmatrix} + i\begin{pmatrix}|\alpha_1|^2 & -\alpha_0\bar{\alpha}_1\\ -\bar{\alpha}_0\alpha_1 & |\alpha_0|^2\end{pmatrix}\right)\right).$$

The answer is obviously negative. It indeed suffices to solve the equation

$$1+i = \langle \mathbf{z}|\left(\left(\begin{pmatrix}0 & 0\\ 0 & 1\end{pmatrix} + i\begin{pmatrix}|\alpha_1|^2 & -\alpha_0\bar{\alpha}_1\\ -\bar{\alpha}_0\alpha_1 & |\alpha_0|^2\end{pmatrix}\right)|\mathbf{z}\rangle,$$

for some $\|\mathbf{z}\| = 1$. Taking the real part of the above implies that $\|z_2\|^2 = 1$; hence $\|z_1\| = 0$. Next, taking the imaginary part implies that $\|z_1\alpha_1 - z_2\alpha_0\|^2 = 1$. It follows that $\|z_2\alpha_0\|^2 = 1$; hence $\|\alpha_0\| = 1$ and $\alpha_1 = 0$, so that the initial and terminal Hamiltonians would be the same, which is an irrelevant situation.

From the overall geometric situation depicted in Fig. 2, it follows that the arguments of the lines passing through $\{1+i\}$ and tangent to the boundary of the ellipse

$$\partial\mathcal{F}\left(\left(\begin{pmatrix}0 & 0\\ 0 & 1\end{pmatrix} + i\begin{pmatrix}|\alpha_1|^2 & -\alpha_0\bar{\alpha}_1\\ -\bar{\alpha}_0\alpha_1 & |\alpha_0|^2\end{pmatrix}\right)\right)$$

are at arguments of $0°$ and $90°$ with the real axis. Hence, even though in theory the critical values do cross, this crossing is, however, not visited by the homotopy $\theta \in (0, \pi/2)$. This theoretically-relevant (but physically irrelevant) crossing is evident from the plots of Fig. 1.

Note that in the quantum adiabatic brachistochrone solution subject to $u_0(t) + u_1(t) = 1,\ t \in [0,1]$, the path is [3,14]

$$u_1(t) = \frac{1}{2} - \frac{|\alpha_0|}{2\sqrt{1-|\alpha_0|^2}}\tan\left((1-2t)\arccos|\alpha_0|\right).$$

It is easily seen that the above is monotone increasing with t and as such the angles visited are all in $[0, \pi/2]$.

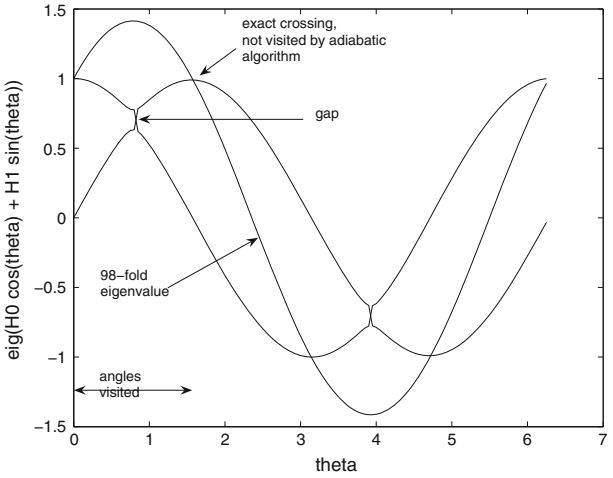

Fig. 1 Plots of eigenvalues of homotopy of Grover's Hamiltonians for $N = 100$ and $m = 39$. Observe that what is indicated as "gap" is a genuine gap; the fact that the curves *appear* to cross is a numerical artifact

3.1 Grover's quantum search algorithm

In Grover's Hamiltonian, we have $|\mathbf{a}\rangle = \sum_{k=0}^{N-1} |k\rangle/\sqrt{N}$ and $|\mathbf{b}\rangle = |m\rangle$, where $m \in \{0, 1, 2, \ldots, N-1\}$, so that $\alpha_0 = 1/\sqrt{N}$.

Figure 1 shows the plots of eigenvalues of $H_0 \cos\theta + H_1 \sin\theta$ for $N = 100$ and $m = 39$. The gap between the ground state and the first excited state is quite obvious and occurs at an angle visited by the adiabatic algorithm. Also observe the *exact* crossing corresponding to the projection of $\mathcal{F}(H_0 + iH_1)$ along the line tangent to $\partial\mathcal{F}\begin{pmatrix} 0 & 0 \\ 0 & 1 \end{pmatrix} + i\begin{pmatrix} |\alpha_1|^2 & -\alpha_0\bar{\alpha}_1 \\ -\bar{\alpha}_0\alpha_1 & |\alpha_0|^2 \end{pmatrix}$ and passing through $1 + i$. This exact crossing corresponds to an angle not visited by the algorithm, as set up in [3,14].

The numerical range of the matrix $H_0 + iH_1$ for the same parameter values ($N = 100$, $m = 39$) is shown in Fig. 2.

3.2 Solving Toeplitz equations

The Hamiltonians for the inversion of a $N \times N$ Toeplitz matrix T are constructed from $|a\rangle = \sum_{k=0}^{N-1} |k\rangle/\sqrt{N}$ and $b = T^{-1}|11\ldots1\rangle/\|T^{-1}|11\ldots1\rangle\|$. Figure 3 shows the plots of eigenvalues for a 10×10 Toeplitz matrix such that $T(1, j) = j$ and $T(i, 1) = i^2$, $i, j = 1, \ldots, 10$. Observe the gap. Also observe that the algorithm is coming dangerously close to the "exact crossing."

3.3 Scaling of the gap

We briefly review how our approach recovers some known results related to the scaling of the gap with the size N of the problem. Define

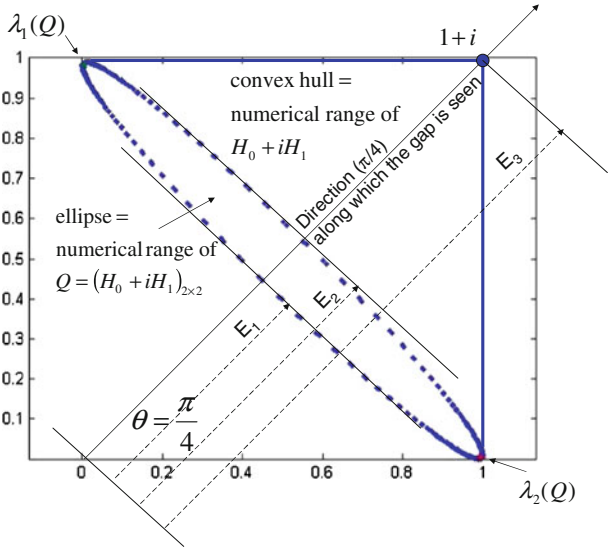

Fig. 2 Numerical range of $H_0 + i\,H_1$ for Grover's search algorithm for $N = 100$ and $m = 39$

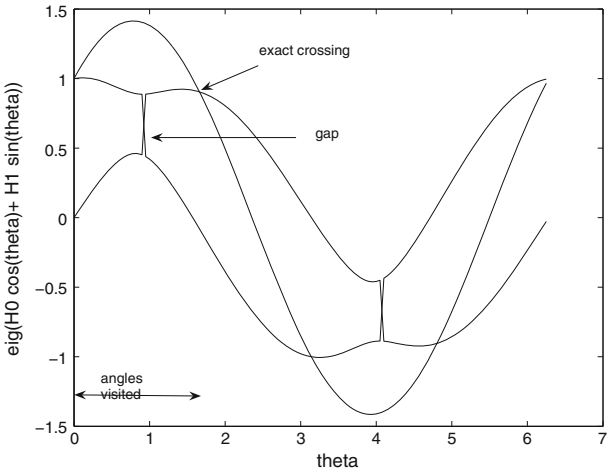

Fig. 3 Plots of eigenvalues of homotopy of Hamiltonians for solving a 10×10 Toeplitz system. As in Fig. 1, the apparent crossing at the gap is a numerical artifact

$$Q = Q_0 + i\,Q_1 = \begin{pmatrix} 0 & 0 \\ 0 & 1 \end{pmatrix} + i \begin{pmatrix} |\alpha_1|^2 & -\alpha_0\bar{\alpha}_1 \\ -\bar{\alpha}_0\alpha_1 & |\alpha_0|^2 \end{pmatrix},$$

so that

$$H_0 + i\,H_1 = Q \oplus (1+i)I_{N-2}.$$

As already said, $\mathcal{F}(H_0 + j\,H_1)$ is the convex hull of $\mathcal{F}(Q)$ and $\{1+i\}$. It is well known that $\mathcal{F}(Q)$ is an ellipse with foci at $\lambda_i(Q)$, $i = 1, 2$, and

$$\text{minor principal axis} = \sqrt{\text{Tr}[Q^*Q] - |\lambda_1(Q)|^2 - |\lambda_2(Q)|^2},$$
$$\text{major principal axis} = \sqrt{\text{Tr}[Q^*Q] - 2\Re(\lambda_1(Q)\bar{\lambda}_2(Q))}.$$

The following lemma is easily proved:

Lemma 1 *That part of $\partial\mathcal{F}(Q)$ in the interior of $\mathcal{F}(H_0 + iH_1)$ is a critical value curve of f; hence, it is the locus of some critical values of $f_\theta(\mathbf{z}) = \langle\mathbf{z}|(H_0\cos\theta + H_1\sin\theta)|\mathbf{z}\rangle$ for $\theta \in [0, 2\pi)$.*

Proof Obviously, that part of $\partial\mathcal{F}(Q)$ in the interior of $\mathcal{F}(H_0 + iH_1)$ is the locus of some eigenvalues of $Q_0\cos(\theta) + Q_1\sin(\theta)$ for some $\theta \in [0, 2\pi)$. Hence it consists of eigenvalues of $H_0\cos(\theta) + H_1\sin(\theta)$ for some θs. Hence it is a critical value of f.

Therefore, the various energy levels $E_1(\theta)$, $E_2(\theta)$, $E_3(\theta)$ are found as the distances between the origin and the tangents to the critical value curves at an argument of $\theta \pm \pi/2$, as shown in Fig. 2 for a specific θ. From the same figure, it is geometrically obvious that the shortest distance between the ground state $E_1(\theta)$ and the first excited state $E_2(\theta)$ is found as the minor principal axis of the ellipse $\partial\mathcal{F}(Q)$.

Therefore, to recover the scaling of the gap in our set-up, it suffices to show that the minor principal axis of $\partial\mathcal{F}(Q)$ closes as $N \to \infty$. It is a matter of simple calculation to derive

$$Q = \begin{pmatrix} i\left(1 - \frac{1}{N}\right) & -i\sqrt{\frac{1}{N} - \frac{1}{N^2}} \\ -i\sqrt{\frac{1}{N} - \frac{1}{N^2}} & 1 + \frac{i}{N} \end{pmatrix}.$$

The characteristic polynomial of the above matrix is found to be

$$s^2 + s(-1 - i) + i(1 - 1/N),$$

from which the eigenvalues are found exactly as

$$\lambda_1(Q) = \frac{1}{2}\left(1 - \sqrt{1 - \frac{2}{N}} + i\left(1 + \sqrt{1 - \frac{2}{N}}\right)\right),$$
$$\lambda_2(Q) = \frac{1}{2}\left(1 + \sqrt{1 - \frac{2}{N}} + i\left(1 - \sqrt{1 - \frac{2}{N}}\right)\right).$$

Therefore, we find

$$|\lambda_1(Q)|^2 = |\lambda_2(Q)|^2 = 1 - 1/N.$$

Next, the Frobenius norm of Q is found via $\text{Tr}[Q^*Q] = 2$. Finally, putting everything together we find the exact gap:

$$\text{principal minor axis} = \text{gap} = \sqrt{2 - 1 + \frac{1}{N} - 1 + \frac{1}{N}} = \sqrt{\frac{2}{N}}. \qquad \square$$

4 Singularity

4.1 Bifurcation to stable singularities

The numerical range depicted in Fig. 2 is a textbook example of a *nongeneric* one. In its simpler formulation, this means that the "sharp point" $1+i$, defined as a point where the boundary is not differentiable, along with the "flat" lines segments joining $1+i$ to the tangency points with the ellipse, do not persist under general data perturbation, no matter how small [9]. Recall from Sect. 2.2 that a matrix $H_0 + iH_1$ is *generic* if the eigenvalues of $H_0 \sin\theta + H_1 \cos\theta$ are all simple for all values of θ and hence do not cross [4, Definition 9]. The set of generic matrices is open and dense in the set of matrices with the usual Euclidean topology on the entries [6, Proposition 4.9]. Sharp points and line segments embedded in the boundary, as they appear in the template of Fig. 2, are among the features disqualifying a matrix from being generic [4, Corollary 3, Theorem 12]. From the differential topology viewpoint, recall that the preimage of the boundary of the numerical range is composed of critical points, which are rank deficient in the sense that $\text{rank}(d_{|\mathbf{z}\rangle} f) \leq 1$ for $|\mathbf{z}\rangle \in f^{-1}(\partial\mathcal{F})$. As a refined classification, $\text{rank}(d_{|\mathbf{z}\rangle} f) = 1$ for a smooth boundary point, whereas $\text{rank}(d_{|\mathbf{z}\rangle} f) = 0$ for a sharp point (see [4, Sec. 3] and [9]).

Under data perturbation, the nongeneric features—the sharp point, the rank 0 property of its preimage, and the line segments in the boundary—are all removed to produce a generic template. The multiple eigenvalue $1+i$ splits into distinct eigenvalues, while at the same time each line segment in the boundary splits, two of them remaining in the boundary while the others combine with the nonboundary part of the ellipse to produce nondifferentiable critical value curves in the interior of the numerical range. Two examples of how Fig. 2 evolves under data perturbation are shown in Figs. 4 and 5. To make the bifurcation process easily visualizable, we restricted ourselves to $N = 4$, in which case the eigenvalue $1+i$ has multiplicity two and bifurcates into two

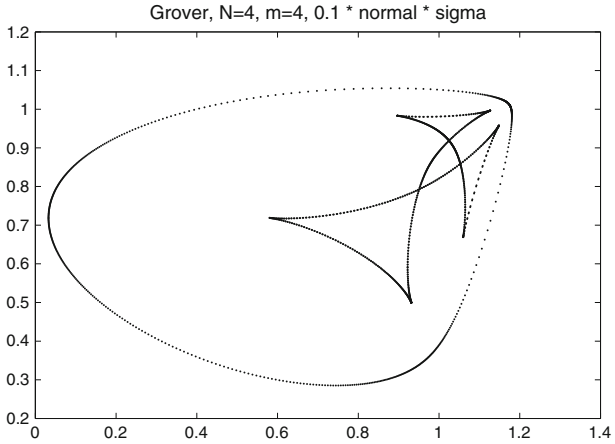

Fig. 4 Numerical range of perturbed $H_0 + iH_1$ for Grover's search algorithm for $N = 4$, $m = 4$, and $\epsilon = 0.1$

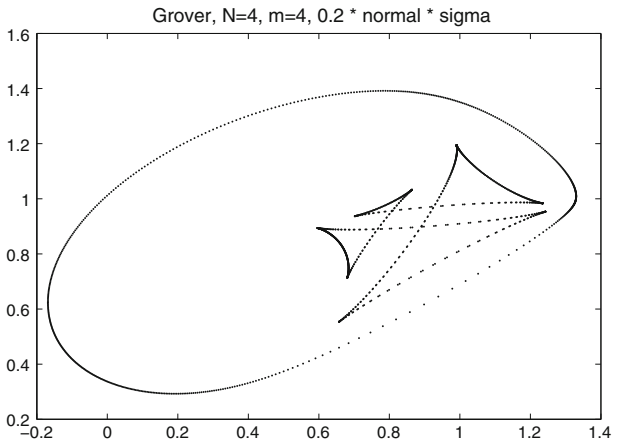

Fig. 5 Numerical range of perturbed $H_0 + iH_1$ for Grover's search algorithm for $N = 4$, $m = 4$, and $\epsilon = 0.2$

eigenvalues, each line segment of the boundary splits into two pieces of curve, one of them remaining in the boundary and the other combining with the nonboundary part of the ellipse to form a nondifferentiable critical value curve in the interior of the numerical range. This curve could have 3 swallow tails with 6 cusps (Fig. 4) or 4 swallow tails with 8 cusps (Fig. 5). In this example, we have made the perturbation somewhat structured, for it to be physically meaningful:

$$\Delta H_0 = \epsilon \sum_q a_{0,q} \sigma_z^{(q)}, \quad \Delta H_1 = \epsilon \sum_q a_{1,q} \sigma_z^{(q)}, \tag{2}$$

where q runs over all qubits, $0 < \epsilon \ll 1$, $a_{0,q}$ and $a_{1,q}$ are numbers chosen uniformly at random in $[-1, 1]$, and $\sigma_z^{(q)}$ is the tensor product of $(q-1)$ times $I_{2\times 2}$ and σ_z in position q.

4.2 Stable singularities

Here we briefly explain how the boundary curve $\partial\mathcal{F}$ is generically smooth, whereas the critical value curves in the interior of $\mathcal{F}$ have singularities. We further show that these singularities are *cusps*, that is, singular points where two critical value branches share a common tangent. A pair of cusps connected by a common critical branch with the two other branches crossing is referred to as *swallow tail* [15]. The motivation for pairing such two cusps in a swallow tail is that the swallow tail can be removed as the two cusp points converge and annihilate each other [15,16]. This reveals a process under which the singular curve of Fig. 5 could bifurcate to that of Fig. 4.

Cusps and swallow tails are *stable* in the sense that they persist under sufficiently small data perturbation. At the precise time when the two cusps of a swallow tail annihilate, the singularity is *unstable* as an arbitrarily small perturbation either reverses to the original swallow tail or removes the singularity altogether.

4.2.1 Cusps

It is convenient to define a critical value curve as the envelope of the θ-parameterized family of lines orthogonal to $e^{i\theta}$ passing through the point $\lambda_k(\theta)e^{i\theta}$, where $\lambda_k(\theta)$ is an eigenvalue of $H(\theta)$. Clearly, the equation of such a line in $x + iy$ coordinates is

$$L(\theta) : (y - \lambda(\theta)\sin\theta) = -\frac{\cos\theta}{\sin\theta}(x - \lambda(\theta)\cos\theta).$$

On the other hand, if $\theta \mapsto u(\theta) + iv(\theta)$ is the parameterization of the critical value curve, the tangent of argument $\theta + \pi/2$ to the point $u(\theta) + iv(\theta)$ is

$$L(\theta) : (y - v(\theta)) = \frac{v'(\theta)}{u'(\theta)}(x - u(\theta)).$$

Equating the two lines yields the equations of the envelope as

$$\frac{\sin\theta}{u'(\theta)} = \frac{\cos\theta}{-v'(\theta)} = \frac{\lambda(\theta)}{-u(\theta)v'(\theta) + v(\theta)u'(\theta)}.$$

Some elementary manipulations yield

$$\lambda(\theta) = v(\theta)\sin\theta + u(\theta)\cos\theta.$$

Before differentiating the above, it is necessary to agree on how to prolong an eigenvalue in case of crossing; precisely, given $\lambda(\theta \le \theta_\times)$ uniquely defined and $\lambda(\theta_\times) = \lambda_1(\theta_\times) = \lambda_2(\theta_\times) = \cdots$ with $\lambda_1(\theta) \ne \lambda_2(\theta) \ne \cdots$ for $\theta \in (\theta_\times, \theta_\times + \epsilon)$, how to define $\lambda(\theta > \theta_\times)$? Even though the eigenvalue $\lambda(\theta_\times)$ is multiple, the equation $\det(H_0\cos\theta + H_1\sin\theta - \lambda(\theta)I) = 0$ can always be resolved into several analytical branches around $\theta_\times$, and $\lambda(\theta \le \theta_\times)$ is prolonged along such a branch. Differentiating the above expression for λ and solving for u, v yields

$$\begin{aligned} u &= \lambda\cos\theta - \lambda'\sin\theta, \\ v &= \lambda\sin\theta + \lambda'\cos\theta. \end{aligned}$$

The above is the equation of the critical value curve in the θ-parameterization.

Differentiating the parameterized equations of the curve yields

$$\begin{aligned} u' &= -(\lambda + \lambda'')\sin\theta, \\ v' &= (\lambda + \lambda'')\cos\theta. \end{aligned}$$

In the $\theta \mapsto \big(u(\theta), v(\theta)\big)$ parameterization, a *singularity* is a point where the tangent vector $\big(u'(\theta), v'(\theta)\big)$ vanishes; a curve without singularities is said to be *regular* [17, Sec. 1.4]. Clearly, we have the following result:

Theorem 1 $\big(u(\theta^0), v(\theta^0)\big)$ *is a singular point of the critical value curve* $\theta \mapsto (u(\theta), v(\theta))$ *iff* $\lambda(\theta^0) + \lambda''(\theta^0) = 0$.

A singular point on a differentiable curve could be either a *corner* or a *cusp* [17, Sec. 1.4], [18, Definition 2.8]. The visually intuitive distinction is that, around a corner, the tangents on either side of the singularity make an angle, while around a cusp the tangent is common. Since $(u'(\theta^0), v'(\theta^0)) = 0$, the θ-parameterization does not provide a tangent. However, recall that, by definition of the envelope, the curve is tangent to the line of argument $\theta + \pi/2$, so that the curve can be given a tangent direction. The ambiguity can also be resolved from

$$\frac{u'}{v'} = -\frac{\sin\theta}{\cos\theta}.$$

The limit as $\theta \to \theta^0$ of the tangent to the curve relative to the θ-parameterization exists and is continuous; thus the tangent is common to both sides of the singularity, which is hence a *cusp*.

A cusp could be of order $3/2$ ($u^2 = v^3$), referred to as *semicubical* cusp, or of order $5/2$ (equivalent after a change of variable to the curve $u^2 = v^5$), also referred to as *ramphoid* cusp. (See [12, Fig. 17] or [19, Fig. 1] for a nice illustration.) Visually, a cusp is a common point to two singular curve branches with a common (Zariski) tangent, with the difference that the $5/2$ cusp has both of its branches on the same side of the tangent to the common point whereas the $3/2$ cusp has its branches on opposite sides of the common tangent [12, Sec. 1.6]. Note that the simplicity of the equation $u^2 = v^5$ might be misleading (see [20, p. 262, Lecture 20]). This can be seen from probably the easiest example of a ramphoid cusp, given by the algebraic curve $(v - u^2)^2 = u^5$ with parameterization $t \mapsto (t^2, t^4 + t^5)$ (see [19, Fig. 1]). By the Whitney theorem, $3/2$ cusps are stable, can be resolved by Nash blowup, whereas $5/2$ cusps cannot be resolved by a single Nash blowup [20, p. 262].

For stable matrices *of even size*, the $3/2$ cusps usually pair in swallow tails, as can be seen from all figures up to now. However, the forthcoming, more complicated case studies reveal somewhat different situations. The Ising chain case of Fig. 8 shows cusps combining to form the vertices of "hyperbolic triangles." This is obviously an unstable situation, as it is shattered by data perturbation. The quantum hitting time of Figs. 9, 10, 11 shows cusps combining to form the vertices of a "rhombus." This situation is not fundamentally different from that of swallow tails; indeed, by "pushing in" two opposite sides of the rhombus until they cross, the cusps pair in swallow tails, a metamorphosis, a "perestroika," anticipated by Arnold [13, Fig. 28].

4.2.2 Boundary versus interior critical value curve

Let $\lambda(\theta)$ be an eigenvalue with normalized eigenvector $|\mathbf{z}(\theta)\rangle$. In [6, Theorem 3.7(3)] it is shown that

$$\lambda''(\theta) = 2\langle \mathbf{z}(\theta)|H'(\theta)(\lambda(\theta)I - H(\theta))^{\dagger}H'(\theta)|\mathbf{z}(\theta)\rangle + \langle \mathbf{z}(\theta)|H''(\theta)|\mathbf{z}(\theta)\rangle,$$

where $H(\theta) = H_0\cos\theta + H_1\sin\theta$. Clearly, $H''(\theta) = -H(\theta)$. Furthermore, $\lambda = \langle \mathbf{z}|H(\theta)|\mathbf{z}\rangle$. Hence,

$$\lambda + \lambda'' = 2\langle \mathbf{z}|H'(\theta)(\lambda I - H(\theta))^{\dagger}H'(\theta)|\mathbf{z}\rangle.$$

The above offers a fresh look at the extra difficulties encountered with the critical value curves inside the numerical range. Order the eigenvalues as $\lambda_1 \leq \lambda_2 \leq \cdots \leq \lambda_N$. On the boundary, $(\lambda_1 I - H(\theta))^\dagger \leq 0$ and $(\lambda_N I - H(\theta))^\dagger \geq 0$, so that the sign of $\lambda_{1,N} - \lambda''_{1,N}$ cannot change with θ, at worst it cancels, and when it cancels it is in the nongeneric case [4]. For all other curves, however, $(\lambda_i I - H(\theta))^\dagger$, $i = 2, \ldots, N-1$, is not sign definite, so that the $\lambda_i + \lambda''_i$ could potentially change sign, hence cancel, and hence create a singularity.

With this new insight, we reformulate a result already available in [4]:

Theorem 2 *If the genericity condition holds, then* $\lambda_1 + \lambda''_1 < 0$ *and* $\lambda_N + \lambda''_N > 0$. *Consequently, the critical value curve with index* $1, N$ *has no singularities.*

Proof It suffices to show that $\lambda_1 + \lambda''_1 \neq 0$. Assume by contradiction that $\lambda_1 + \lambda''_1 = 0$, that is, $2\langle \mathbf{z}|H'(\theta)(\lambda_1 I - H(\theta))^\dagger H'(\theta)|\mathbf{z}\rangle = 0$. Since $\lambda_1 I - H(\theta) \leq 0$, for the latter equality to hold, it is necessary that $|\mathbf{z}\rangle$ be an eigenvector of $H'(\theta)$, say, $H'(\theta)|\mathbf{z}\rangle = \mu|\mathbf{z}\rangle$. Combining the latter with $H(\theta)|\mathbf{z}\rangle = \lambda|\mathbf{z}\rangle$, it is not hard to see that $|\mathbf{z}\rangle$ is an eigenvector of both $H_0 + iH_1$ and $(H_0 + iH_1)^*$. But the latter is not a generic situation [4], hence a contradiction. The proof of $\lambda_N + \lambda''_N > 0$ is the same and left to the reader. □

5 Application to the Ising chain

The Grover search algorithm and the inversion of Toeplitz matrices are well understood examples of adiabatic computations. As such, there is a need to examine the relevance of the numerical range approach to the adiabatic gap in the light of less trivial examples. Among such nontrivial case studies, one will retain the adiabatic computation of the ground state of a transverse Ising chain, in which case the terminal Hamiltonian is

$$H_1 = \sum_{p,q=1}^{n} J_{p,q}\sigma_z^{(p)}\sigma_z^{(q)} + \sum_{q=1}^{n} c_q \sigma_z^{(q)}.$$

The initial Hamiltonian is set up as

$$H_0 = \sum_{q=1}^{n} d_q \sigma_x^{(q)}.$$

$\sigma_z^{(q)}$ is the tensor product of $(N-1)$ identity operators I_2 and the Pauli operator σ_z in position q; $J_{p,q}$ is the coupling strength between spins p and q; the coefficients c_q and d_q are related to the strengths of the magnetic fields along the z and x directions, respectively. As is well known, the linear term in H_1 complicates the problem to the point of making it NP-complete [2].

A significant difference between the preceding cases studies and the present one is that in the former the gap scales as $O(\sqrt{2/N})$ while in the latter it scales as $O\left(1/\log_2 N\right)$.

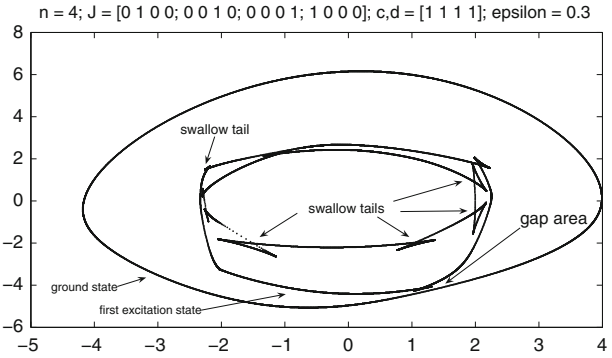

Fig. 6 Numerical range relevant to adiabatic ground state computation of cyclic Ising chain with 4 qubits. Only the ground state boundary curve and the critical value curve getting closest to the boundary (first excitation state) are drawn

As before, we are facing the problem that the nominal numerical range, that is, the numerical range of $H_0 + i\,H_1$, is highly nongeneric, making its interpretation difficult. As in the preceding singularity analysis, we introduce "physically relevant" perturbations in both H_0 and H_1 to break the nongenericity and to force the singularities of the numerical range to bifurcate to stable ones [8], as was already done in Sect. 4.1.

5.1 4-Spin cyclic Ising chain

In this first case, we take $n = 4,\ c_q = d_q = 1,\ \forall q$, with a coupling matrix

$$J = \begin{pmatrix} 0 & 1 & 0 & 0 \\ 0 & 0 & 1 & 0 \\ 0 & 0 & 0 & 1 \\ 1 & 0 & 0 & 0 \end{pmatrix}.$$

To make the singularities of the numerical range easily visualizable, we introduce the perturbation of Eq. (2) with $\epsilon = 0.3$. The results are shown in Fig. 6, where, for the sake of clarity, we have restricted ourselves to two critical value curves: the boundary one (ground state) and the one that gets closest to the boundary (first excitation state).

As already said, the external boundary curve is smooth, while the critical value curve inside the numerical range exhibits singularities of the *swallow tail* type. Recall that the energy levels at some point t along the homotopy are given by the distances between the origin and the tangents at an argument of $\theta(t) \pm \pi/2$ to the various critical value curves. The energy levels would be displayed on the line of argument $\theta(t)$ with the ground level at the intersection of the argument $\theta(t)$ line and the tangent to the boundary. From Fig. 6, it follows that the gap occurs between the boundary curve and a swallow tail. The latter explains the discrepancy between the simple cases where the problem can be reduced to the direct sum of a 2×2 matrix and a scalar matrix and the present case.

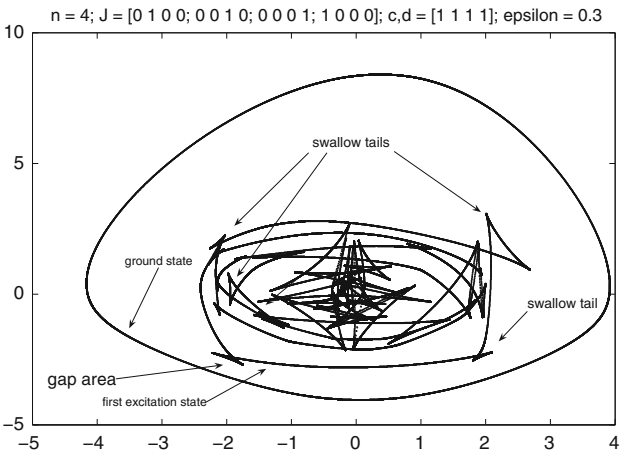

Fig. 7 Numerical range relevant to adiabatic ground state computation of cyclic Ising chain with 4 qubits. All critical value curves (corresponding to all energy levels) are drawn

To be complete, we considered the same problem, but we plotted *all* critical value curves, as shown in Fig. 7. While the data is essentially the same as that of Fig. 6, the random perturbation ($\epsilon = 0.3$) creates a difference between the two figures, although the similarity between the ground state curve and the first excitation state curve is obvious. In this case, for any look-up angle θ, there should be exactly 2^4 tangents at the angle θ to the critical values curves. These represent the 16 energy levels.

It is also instructive to look at the *unperturbed* ($\epsilon = 0$) case. In this case, the problem has complete symmetry and the gap closes. Not surprisingly, the (complete) critical value set also has symmetry, as shown in Fig. 8. Another problem is that because of the nongenericity of the problem some critical value curves do not show very clearly (look at the vertical "dots" at $\Re = \pm 2$).

6 Application to quantum hitting time of Markov chains

Here we consider yet another quantum adiabatic gap problem amenable to the numerical range analysis—hitting one of the "marked" states in a Markov chain [21,22]. It somewhat departs from the main stream of applications considered thus far, in the sense that it involves a reversal of the critical value curves: the ground state is the origin of $\mathbb{C}$ and the maximum excitation state is the boundary of the template. Furthermore, this case study reveals singularities never seen before.

6.1 Review

We consider a $n \times n$ Markov state transition (row stochastic) matrix

$$P_0 = \begin{pmatrix} P_{UU} & P_{UM} \\ P_{MU} & P_{MM} \end{pmatrix},$$

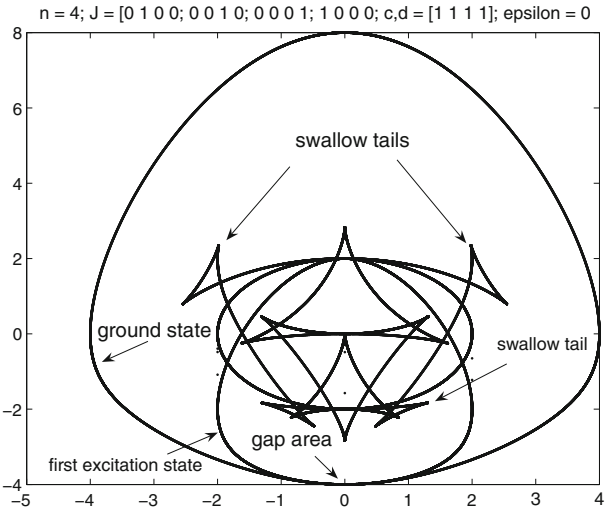

Fig. 8 Numerical range relevant to adiabatic ground state computation of cyclic Ising chain with 4 qubits, in the symmetric, unperturbed case, with the gap closing. All critical value curves (corresponding to all energy levels) are drawn. Observe the unstable combination of cusps in "hyperbolic triangles"

where the partition of the matrix is relative to the "marked" (M) versus the "unmarked" (U) states. There are m marked states. This Markov chain is assumed to be ergodic, that is, the eigenvalue 1 is unique. The problem is to hit a marked state as efficiently as possible through a quantum random walk [21]. Once a marked state is hit, the Markov chain stays at the marked state that has been hit, that is, the Markov state transition matrix becomes

$$P_1 = \begin{pmatrix} P_{UU} & P_{UM} \\ 0 & I_{m\times m} \end{pmatrix}.$$

Observe that this new Markov chain is not ergodic, unless $m = 1$. The adiabatic homotopy from P_0 to P_1 is, in our set-up, parameterized as

$$P(\theta) := P_0 \cos\theta + P_1 \sin\theta = \begin{pmatrix} P_{UU}(\cos\theta + \sin\theta) & P_{UM}(\cos\theta + \sin\theta) \\ P_{MU}\cos\theta & P_{MM}\cos\theta + I_{m\times m}\sin\theta \end{pmatrix}.$$

In this parameterization, the "initial" state is $\theta = 0$ ($s = 0$ in the notation of [22]) and the "terminal" state corresponds to $\theta = \pi/2$ ($s = 1$ in the notation of [22]). Observe that, here, the path is not the same as that of [22]. In addition, consistently with our approach, we need to construct a return path from $\theta = \pi/2$ back to $\theta = 2\pi$. The classical discriminant of the detailed balance is given by

$$D(\theta) = \sqrt{P(\theta) * P(\theta)^T},$$

where $*$ denotes the entrywise (Schur or Hadamard) product and $\sqrt{\cdot}$ denotes the entrywise square-root. The eigenvalues of the discriminant are ordered as[1]

$$0 \leq \lambda_1(\theta) \leq \lambda_2(\theta) \leq \cdots \leq \lambda_n(\theta) = 1. \tag{3}$$

The crucial step is to map the classical walk to the Hamiltonian of a quantum walk

$$H(\theta) : \mathbb{C}^n \otimes \mathbb{C}^n \to \mathbb{C}^n \otimes \mathbb{C}^n,$$

defined via the eigenvectors $v_k(\theta)$ and eigenvalues $\lambda_k(\theta)$, $k = 1, \ldots, n$, of the discriminant $D(\theta)$, together with an arbitrary reference state $|0\rangle$ in the second factor of $\mathbb{C}^n \otimes \mathbb{C}^n$, as

$$H(\theta)|v_k(\theta), 0\rangle = i\sqrt{1 - \lambda_k^2(\theta)}|v_k(\theta), 0\rangle^{\perp_\theta}, \tag{4}$$

$$H(\theta)|v_k(\theta), 0\rangle^{\perp_\theta} = -i\sqrt{1 - \lambda_k^2(\theta)}|v_k(\theta), 0\rangle. \tag{5}$$

Here $|v_k(\theta), 0\rangle^{\perp_\theta}$ is a section through the orthogonal complement $|v_k(\theta), 0\rangle^{\perp}$, that is, a single vector picked up θ-continuously in $|v_k(\theta), 0\rangle^{\perp}$.[2] In [22], the path is from $\theta = 0$ to $\theta = \pi/2$, so that the base space $[0, \pi/2]$ is contractible and the section exists. Here, however, the loop is closed by a path from $\pi/2$ to 2π, so that the base space S^1 is not contractible, and this raises the question of existence of the section:

Lemma 2 *If the eigenvalues of $D(\theta)$ are pairwise distinct, the section $\left\{|v_k(\theta), 0\rangle^{\perp_\theta} : k = 1, \ldots, n-1\right\}$ exists over S^1.*

Proof First, observe that existence of the $SU(n)$-section $\{|v_k(\theta)\rangle : k = 1, \ldots, n\}$ is guaranteed as the set of θ-dependent orthonormalized eigenvectors of the Hermitian operator $D(\theta)$ under the no eigenvalue crossing condition. Existence of the section $\left\{|v_k(\theta), 0\rangle^{\perp_\theta} : k = 1, \ldots, n-1\right\}$ is a fact of stable homotopy theory, as the section exists because there is "enough space" in $\mathbb{C}^n \otimes \mathbb{C}^n$. Precisely, try $|v_k(\theta), 0\rangle^{\perp_\theta} = |v_k(\theta), w_k(\theta)\rangle$. We must secure $(|v_k(\theta), 0\rangle, |v_k(\theta), w_k(\theta)\rangle) = 0$. Since

$$(|v_k(\theta), 0\rangle, |v_k(\theta), w_k(\theta)\rangle) = (|v_k(\theta)\rangle, |v_k(\theta)\rangle)\,(|0\rangle, |w_k(\theta)\rangle)\,, \tag{6}$$

it suffices to take w_k such that $(|0\rangle, |w_k(\theta)\rangle) = 0$. Take the $(n-1)$-dimensional subspace of $\mathbb{C}^n$ orthogonal to $|0\rangle$, take the orthonormal set $\{w_k(\theta) : k = 1, \ldots, n-1\}$

[1] Securing nonnegativity of the eigenvalues might require replacing P by $(P + I)/2$, which only affects the hitting time by a factor of 2 (see [22, V.A]).

[2] $|v_k(\theta), 0\rangle$ denotes the tensor product of $v_k(\theta)$ and the reference state in the second factor of $\mathbb{C}^n \otimes \mathbb{C}^n$, but we refrain from using the notation $v_k(\theta) \otimes 0$, as it could be confused with 0.

in that subspace by, say, the Gram-Schmidt process leaving the w_k's independent of θ. $\{|v_k(\theta), w_k\rangle : k = 1, \ldots, n-1\}$ is one possible required section. □

We temporarily restrict ourselves to $\theta \in [0, \pi/2)$ ($s \in [0, 1)$ in the notation of [22]) as there is a continuity issue at $\theta = \pi/2$. Equation (4) defines the Hamiltonian $H(\theta)$ over the space

$$V(\theta) = \operatorname{span}\left\{\left(|v_1(\theta), 0\rangle, |v_1(\theta), 0\rangle^{\perp_\theta}\right), \ldots, \left(|v_{n-1}(\theta), 0\rangle, |v_{n-1}(\theta), 0\rangle^{\perp_\theta}\right), |v_n(\theta), 0\rangle\right\}.$$

Observe the following:

Lemma 3 $\dim_{\mathbb{C}}(V(\theta)) = 2n - 1$.

Proof Consider the two subspaces:

$$\begin{aligned} V_1 &= \operatorname{span}\{\ |v_1(\theta), 0\rangle\ , \ldots, |v_{n-1}(\theta), 0\rangle\ , |v_n(\theta), 0\rangle\ \}, \\ V_2 &= \operatorname{span}\{\ |v_1(\theta), 0\rangle^{\perp_\theta}\ , \ldots, |v_{n-1}(\theta), 0\rangle^{\perp_\theta}\ ,\ \ \}. \end{aligned}$$

Each of the above two subspaces is maximal dimensional ($\dim V_1 = n$ and $\dim V_2 = (n-1)$). Moreover, they are mutually orthogonal ($V_1 \perp V_2$). Hence the result. □

Over the orthogonal complement, $V(\theta)^\perp$, the Hamiltonian vanishes [22, V.B]. The Hamiltonian $H(\theta)$, $\theta \in [0, \pi/2)$, is given by

$$\begin{aligned} &H(\theta) = \\ &-\begin{pmatrix} V(\theta) & | & V(\theta)^\perp \end{pmatrix} \\ &\cdot \left(\begin{array}{cccc|c} \sqrt{1-\lambda_1^2(\theta)}\sigma_y & \cdots & 0_{2\times 2} & 0_{2\times 1} & 0_{2\times(n-1)^2} \\ 0_{2\times 2} & \cdots & 0_{2\times 2} & 0_{2\times 1} & 0_{2\times(n-1)^2} \\ \vdots & \ddots & \vdots & \vdots & \vdots \\ 0_{2\times 2} & \cdots & \sqrt{1-\lambda_{n-1}^2(\theta)}\sigma_y & 0_{2\times 1} & 0_{2\times(n-1)^2} \\ 0_{1\times 2} & \cdots & 0_{1\times 2} & 0 & 0_{1\times(n-1)^2} \\ \hline 0_{(n-1)^2\times 2} & \cdots & 0_{(n-1)^2\times 2} & 0_{(n-1)^2\times 1} & 0_{(n-1)^2\times(n-1)^2} \end{array}\right) \\ &\cdot \begin{pmatrix} V(\theta) & | & V(\theta)^\perp \end{pmatrix}^*. \end{aligned}$$

The terminal ($s = 1$ in the notation of [22]) Hamiltonian is

$$
\begin{aligned}
&H(\frac{\pi}{2}) = \\
&-\left(V(\tfrac{\pi}{2}) \;\mid\; V(\tfrac{\pi}{2})^{\perp}\right) \\
&\cdot\left(\begin{array}{cccc|c}
\sqrt{1-\lambda_1^2(\frac{\pi}{2})}\sigma_y & \dots & 0_{2\times 2} & 0_{2\times(2m-1)} & 0_{2\times(n-1)^2} \\
0_{2\times 2} & \dots & 0_{2\times 2} & 0_{2\times(2m-1)} & 0_{2\times(n-1)^2} \\
\vdots & \ddots & \vdots & \vdots & \vdots \\
0_{2\times 2} & \dots & \sqrt{1-\lambda_{n-m}^2(\frac{\pi}{2})}\sigma_y & 0_{2\times(2m-1)} & 0_{2\times(n-1)^2} \\
0_{(2m-1)\times 2} & \dots & 0_{(2m-1)\times 2} & 0_{(2m-1)\times(2m-1)} & 0_{(2m-1)\times(n-1)^2} \\
\hline
0_{(n-1)^2\times 2} & \dots & 0_{(n-1)^2\times 2} & 0_{(n-1)^2\times(2m-1)} & 0_{(n-1)^2\times(n-1)^2}
\end{array}\right) \\
&\quad\cdot\left(V(\tfrac{\pi}{2}) \mid V(\tfrac{\pi}{2})^{\perp}\right)^{*}.
\end{aligned}
$$

In both of the above, σ_y is the usual Pauli operator $\begin{pmatrix} 0 & i \\ -i & 0 \end{pmatrix}$.

By Lemma 2, a return path from $\pi/2$ to 2π exists and could be obtained by some extension of $H(\theta)$ from $[0, \pi/2)$ to $[0, 2\pi)$. Here, however, for the sake of simplicity and to be consistent with our objective of exhausting all singularities that could be encountered along all paths, including the one of [22], the homotopy and the return path are set up as $H_0 \cos\theta + H_1 \sin\theta$, $\theta \in [0, 2\pi)$, where $H_0 = H(0)$ and $H_1 = H(\pi/2)$. The relevant numerical range is the one of the matrix $H_0 + iH_1$. Observe that this matrix can be rewritten as

$$
\begin{aligned}
&H_0 + iH_1 = \\
&\quad V(0)\mathrm{diag}\left\{\sqrt{1-\lambda_k(0)}\sigma_y : k = 1, \dots, n-1; 0\right\} V(0)^* \\
&\quad + iV\left(\frac{\pi}{2}\right)\mathrm{diag}\left\{\sqrt{1-\lambda_k\left(\frac{\pi}{2}\right)}\sigma_y : k = 1, \dots, n-m; 0_{(2m-1)\times(2m-1)}\right\} V\left(\frac{\pi}{2}\right)^* \\
&\quad \oplus 0_{(n-1)^2\times(n-1)^2}.
\end{aligned}
$$

In the numerical simulations, only the first two terms will be considered, as the third term is just a multiple point 0 in the numerical range.

The adiabatic condition invoked in [22, Eq. (34)] is the "folk" condition

$$
\sum_{k=1}^{n-1} \frac{|\langle\psi_k(t)|\dot{\psi}(t)\rangle|^2}{(E_k(t) - E_n(t))^2} \ll 1, \quad \forall t \in [0, 1],
$$

rather the *exact* condition of the Introduction. Nevertheless, the fundamental feature that the gaps

$$
E_k(\theta) - E_n(\theta) = \sqrt{1-\lambda_k^2(\theta)} - 0,
$$

where the E_k's are the energy levels and $E_n = 0$ is the ground state, are the limiting factors for adiabatic behavior remains the same.

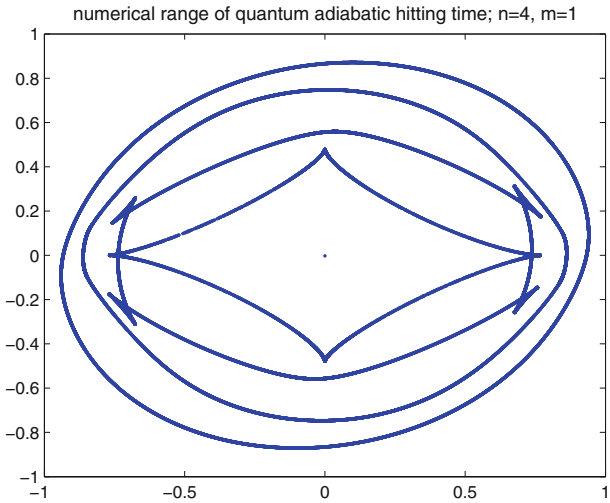

Fig. 9 $n = 4,\ m = 1$ case. Observe that the first excitation state is an ideal rhombus, with its cusps not pairing in swallow tails. The gap is obtained as the minimum of all θ-gaps as θ rotates

6.2 Simulations

In the simulations, we took P to be a doubly stochastic matrix generated by the subroutine `magic` of Matlab. The reference state $|0\rangle$ was here taken as $e_1 = \begin{pmatrix} 1 & 0 & \dots & 0 \end{pmatrix} \in \mathbb{C}^n$. Next, we picked $w_k = e_{k+1},\ k = 1, 2, \dots, n-1$, where $e_k,\ k = 1, \dots, n$ is the natural basis of $\mathbb{C}^n$ over $\mathbb{C}$. Recall that $|v_k, 0\rangle^{\perp}$ is chosen as $|v_k, w_k\rangle$. We computed the numerical range of $H_0 + i\,H_1$ and its critical value curves for various n and various m. All numerical ranges are symmetric relative to $0 + i0$. The gap is thus the smallest distance between two parallel lines: one passing through $0 + i0$, the critical value of the ground level E_n, and the other tangent to the E_{n-1} critical value curve.

6.2.1 Case $n = 4,\ m = 1$

The results are shown in Fig. 9. The remarkable thing is that in addition to four swallow tails made up of $3/2$ cups one has four cusps of the semicubical type, that is, the critical value branches are on either side of the common tangent.

6.2.2 Case $n = 6,\ m = 2$

The results are shown in Fig. 10.

6.2.3 Case $n = 7,\ m = 2$

The results are shown in Fig. 11.

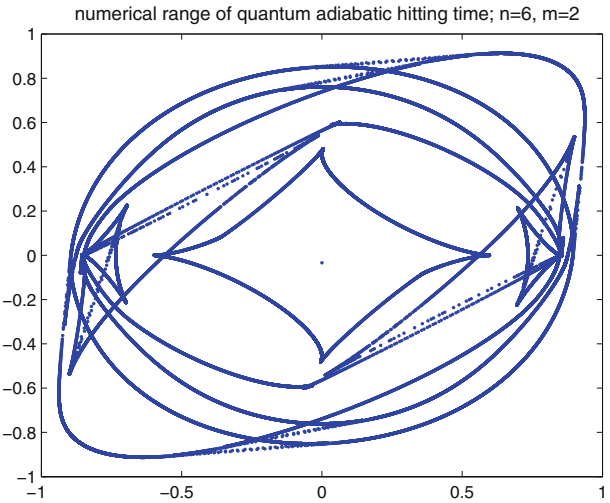

Fig. 10 $n = 6,\ m = 2$ case. Observe that the first excitation state is still an ideal rhombus

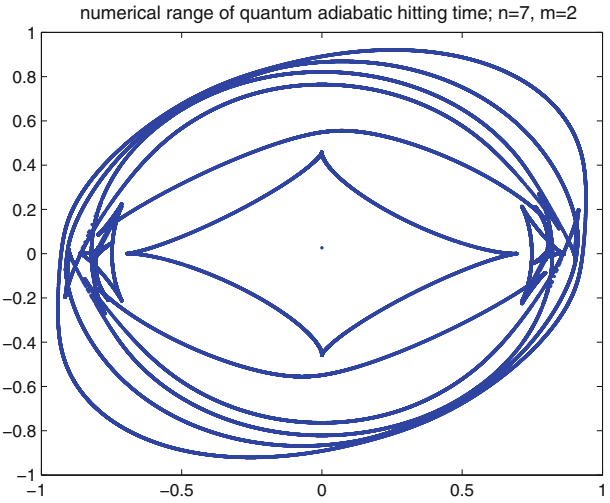

Fig. 11 $n = 7,\ m = 2$ case. Observe that the first excitation state is still an ideal rhombus

7 Conclusion: towards navigation in a maze of singularities

We have shown that under an adiabatic homotopy between two Hamiltonians, we are likely to encounter singularities that create the "gap," requiring a slow-down of the process through the gap. These singularities manifest themselves as near crossings of eigenvalues of $H_0u_0(t) + H_1u_1(t)$ or, as argued in the present paper, as pairs of critical value curves of the quadratic mapping of $H_0 + i\,H_1$ getting dangerously close, a phenomenon that is inextricably intertwined with swallow tails developing precisely in the area of close encounter between the two critical value curves. A brachistochrone

solution that satisfies the adiabatic condition and skillfully navigates "around" the singularities has already been proposed [14]. However, another solution, closer to the spirit of understanding the differential topology of the singularities, would attempt to leave the plane span(H_0, H_1) in the space of Hermitian operators and "jump" over the singularity. This process, however, would need a higher number of control parameters, with the inevitable consequence that the higher the number of control parameters the more singularities could develop, even singularities translating to *exact* crossing, a phenomenon already singled out by von Neumann. The remaining challenge is to find the trade-off between adding control parameters and keeping the singularity structure manageable.

Acknowledgments E.A.J. was partially supported by the Army Research Office (ARO) Multi University Research Initiative (MURI) grant W911NF-11-1-0268. A.T.R. acknowledges the support of the USC Center for Quantum Information Science & Technology, where part of this work was completed. The authors wish to thank Dr. D. Lidar for helpful discussions on the material of this paper.

References

1. Sarandy, M.S., Wu, L.A., Lidar, D.A.: Consistency of the adiabatic theorem. Quantum Inf. Process. **3**, 331 (2004)
2. Lidar, D.A., Rezakhani, A.T., Hamma, A.: Adiabatic approximation with exponential accuracy or many-body systems and quantum computation. J. Math. Phys. **50**, 102106 (2009)
3. Rezakhani, A.T., Pimachev, A.K., Lidar, D.A.: Accuracy versus run time in an adiabatic quantum search. Phys. Rev. A **82**, 052305 (2010)
4. Jonckheere, E.A., Ahmad, F., Gutkin, E.: Differential topology of numerical range. Linear Algebra Appl. **279**(1-3), 227 (1998)
5. Neumann, J.von , Wigner, E.: Uber das Verhalten von Eigenwerten bei adia-balischen Prozessen. Phys. Zschr. **30**, 467 (1929)
6. Gutkin, E., Jonckheere, E.A., Karow, M.: Convexity of the joint numerical range: topological and differential geometric viewpoints. Linear Algebra Appl. LAA **376**, 143 (2003)
7. Jonckheere, E., Shabani, A., Rezakhani, A.: 4th International Symposium on Communications, Control, and Signal Processing (ISCCSP'2010) (Limassol, Cyprus, 2010), Special Session on Quantum Control I. ArXiv:1002.1515v2
8. Golubitsky, M., Guillemin, V.: Stable Mappings and Their Singularities, Graduate Texts in Mathematics, vol. 14. Springer, New York (1973)
9. Ahmad, F.: Differential topology of numerical range and robust control analysis. Ph.D. thesis, Department of Electrical Engineering, University of Southern California (1999)
10. Arnold, V.I., Gusein-Zade, S.M., Varchenko, A.N.: Singularities of Differentiable Maps—The Classification of Critical Points, Caustics and Wave Fronts, vol. 1. Birkhäuser, Boston (1985)
11. Arnold, V.I., Gusein-Zade, S.M., Varchenko, A.N.: Singularities of Differentiable Maps —Monodromy and Asymptotics of Integrals, vol. 2. Birkhäuser, Boston (1988)
12. Arnold, V.I.: The theory of singularities and its applications. Accademia Nationale Dei Lincei; Secuola Normale Superiore Lezioni Fermiane. Press Syndicate of the University of Cambridge, Pisa, Italy (1993)
13. Arnold, V.: Topological invariants of plane curves and caustics, University Lecture Series; Dean Jacqueline B. Lewis Memorial Lectures, Rutgers University, vol. 5. American Mathematical Society, Providence, RI (1994)
14. Rezakhani, A.T., Kuo, W.J., Hamma, A., Lidar, D.A., Zanardi, P.: Quantum adiabatic brachistochrone. Phys. Rev. Lett. **103**, 080502 (2009)
15. Cerf, J.: Publications Mathématiques, Institut des Hautes Etudes Scientifiques (I.H.E.S.) (39), p. 5 (1970)
16. Jonckheere, E.A.: Algebraic and Differential Topology of Robust Stability. Oxford University Press, New York (1997)

17. O'Neill, B.: Elementary Differential Geometry. Academic Press, London (1997)
18. do Carmo, M.P.: Riemannian Geometry. Birkhauser, Boston (1992)
19. Diaz, F.S., Nuno-Ballestros, J.: Plane curve diagrams and geometrical applications. Q. J. Math. **59**, 1 (2007). doi:10.1093/qmath/ham039
20. Harris, J.: Algebraic Geometry–A First Course. Springer, New York (1992)
21. Kempe, J.: Quantum random walks—an introductory overview. Contemp. Phys. **44**(4), 307 (2003)
22. Krovi, H., Ozols, M., Roland, J.: Adiabatic condition and the quantum hitting time of Markov chains. Phys. Rev. A **82**, 1–022333 (2010)